ELSEVIER

Journal of Photochemistry and Photobiology A: Chemistry 141 (2001) 1–7

Journal of Photochemistry and Photobiology A:Chemistry

www.elsevier.nl/locate/jphotochem

Photoinduced electron transfer between fullerenes (C_{60}/C_{70}) and disubstituted naphthalenes using laser flash photolysis

Mohamed El-Khouly [a], Mamoru Fujitsuka [a], Osamu Ito [a,1], Maged El-Kemary [b,*]

[a] *Institute for Chemical Reaction Science, Tohoku University, Katahira, Aoba-ku, Sendai 980-8577, Japan*
[b] *Chemistry Department, Faculty of Education, Tanta University, Kafr El-Sheikh, Egypt*

Received 31 October 2000; received in revised form 1 February 2001; accepted 12 March 2001

Abstract

Photoinduced electron-transfer processes between fullerenes C_{60}/C_{70} and disubstituted-naphthalenes have been studied by laser flash photolysis. Quantum yields (Φ_{et}^{T}) and rate constants (k_{et}) of electron transfer from naphthalenes to the excited triplet states of C_{60} ($^3C_{60}^*$) and C_{70} ($^3C_{70}^*$) have been determined by observing the transient absorption bands in the wide wavelength VIS/NIR regions. The observed Φ_{et}^{T} and k_{et} values depend significantly on the nature and position of the substituents. The k_{et} values are seen to correlate well with the free energy changes (ΔG_{et}) for the electron transfer reactions on the basis of Rehm–Weller relation. Addition of pyridine (Py) enhanced significantly the rates and efficiencies of photoinduced electron transfer process of dihydroxy-naphthalenes (DHN). However, the effect of Py in the dimethoxy-naphthalenes (DMN) is far less than that of DHN. In the presence of octylviologen (OV^{2+}), electron-mediation occurs from $C_{60}^{\bullet -}$ to OV^{2+} to generate $OV^{\bullet +}$.

Keywords: Naphthalenes; Fullerenes; Photoinduced electron transfer; Triplet state

1. Introduction

Photoinduced electron transfer has been attracting considerable attention as one of the most fundamental reactions, because of its crucial roles in a number of chemical and biochemical processes. In spite of enormous photoinduced electron transfer investigations of fullerenes (C_{60}/C_{70}) with various kinds of electron donors [1–4], there have been a few studies concerning the photoinduced electron transfer with di-substituted naphthalene. Linschitz and co-workers [5–7] found that photoinduced electron transfer from phenols and naphthols to C_{60} was strongly enhanced when pyridines were added to polar solution. In our previous investigations, we have reported the electron transfer efficiencies to $^3C_{60}^*$/$^3C_{70}^*$ from mono-substituted naphthalenes [8]. In addition, we had reported that, in both presence and absence of pyridine, the electron transfer efficiencies (Φ_{et}) were confirmed to decrease on going from planer 2-naphthols to perpendicular binaphthols [9].

In this paper, we use the transient absorption techniques in VIS/NIR regions to study the photoinduced electron transfer of C_{60}/C_{70} with different substituted-naphthalene, i.e. dimethoxy-naphthalene (DMN), dihydroxy-naphthalene (DHN) and diamino-naphthalene (DAN). We examine the influence of the substituents on the rates and efficiencies of electron transfer process.

2. Experimental

C_{60} (99.9%) and C_{70} (99.5%) were purchased from Texas fullerene corp. and were used without further purification. Commercial samples of naphthalene, 1-methoxy-napthalene (1-MN), 2-methoxy-naphthalene (2-MN), 2,3-dimethoxy-naphthalene (2,3-DMN), 2,7-dimethoxy-naphthalene (2,7-DMN), 2,3-diaminonaphthalene (2,3-DAN) and 1,8-diamino-naphthalene (1,8-DAN) were purchased from Aldrich. 1,4- and 1,8-dimethoxy-naphthalene (DMN) were prepared using phase transfer catalysis [10] and purified by column chromatography (alumina) followed by vacuum sublimation. Octylviologen OV^{2+} perchlorate was prepared from its chloride. All solvents used were of spectroscopic or HPLC grade.

Nanosecond transient absorption spectra and time profiles were measured using laser photolysis apparatus with a Nd:YAG laser (OPO; 6 ns fwhm) as an exciting source. For the short timescale transient absorption in the near-IR region, a Ge-APD module (Hamamatsu, C5331) was used to monitor the light from a pulsed Xe lamp [11]. For long

* Corresponding author. Fax: +81-298-61-4487.
E-mail address: elkemary@yahoo.com (M. El-Kemary).
[1] Co-corresponding author.

1010-6030/01/$ – see front matter
PII: S1010-6030(01)00430-0

timescale measurements, an InGaAs-PIN detector was used for monitoring the light from continuous Xe-lamp.

Steady-state absorption measurements were carried out using an optical cell (1 cm) with a Shimadzu 2450 UV/VIS spectrophotometer. The solutions of C_{60}/C_{70} and all disubstituted naphthalene were deaerated by Ar-bubbling for 15 min before measurements. All measurements were carried out at 23°C.

3. Results and discussion

3.1. Steady-state UV/VIS spectra

From Fig. 1 it is apparent that the steady-state UV/VIS absorption spectrum of C_{60} in the presence of 1,8-DMN in benzonitrile solvent was similar to the individual absorption spectra of the components. This indicates that there is no ground state interaction between C_{60} and 1,8-DMN under the concentration range used for laser flash photolysis in this study. Similar observations were also made in the case of C_{70} and also for other disubstituted-naphthalenes used in the present study. Throughout our experiments, the fullerenes were predominantly excited by 532 nm laser light since the disubstituted-naphthalene derivatives have no absorbance at this wavelength.

3.2. Transient absorption spectra of C_{60}/C_{70} with naphthalene derivatives

In Fig. 2, we show the transient absorption spectra in the VIS/NIR region obtained by long time-scale nanosecond laser flash photolysis of C_{60} (0.1 mM) with 532 nm light in the presence of 1,8-DMN (20 mM) in deaerated benzonitrile. The transient absorption band at 740 nm is attributed to the triplet–triplet absorption of $^3C_{60}^*$ [1,12–15]. With the decay of $^3C_{60}^*$, a new absorption band appears at 1080 nm with a shoulder at 900 nm; both absorption bands are assigned to the absorption of $C_{60}^{\bullet-}$ [16–19].

The observed time profiles of the absorption bands are shown in the inset of Fig. 2. The decay of $^3C_{60}^*$ at 740 nm,

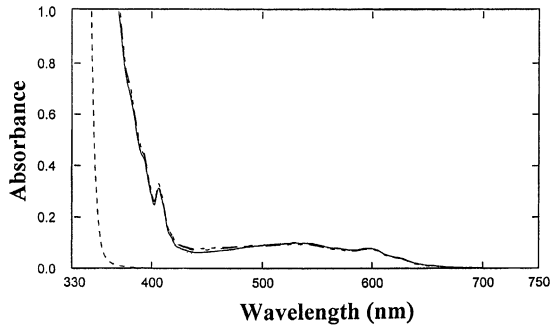

Fig. 1. Steady-state absorption in the UV/VIS region of (—) C_{60} (0.1 mM), (---) 1,8-DMN (20 mM) and their mixture (– –) in the absence and (–·–) presence of Py (0.5 M) in benzonitrile.

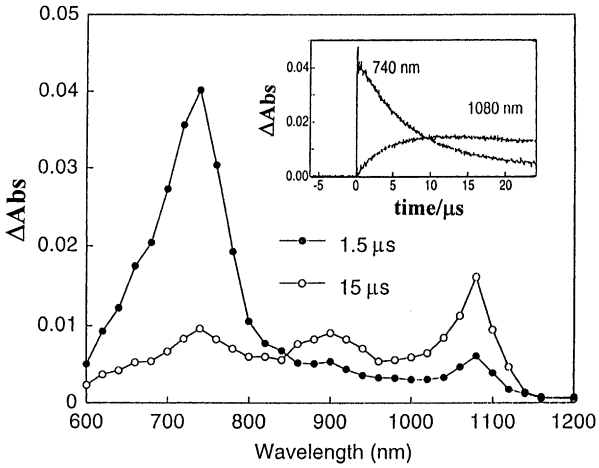

Fig. 2. Transient absorption spectra obtained by 532 nm laser photolysis of C_{60} (0.1 mM) in the presence of 1,8-DMN (20 mM) in Ar-saturated benzonitrile. Inset shows time profiles.

which did not show appreciable decay over a few microsecond without 1,8-DMN, was accelerated in the presence of 1,8-DMN (20 mM). With the decay of $^3C_{60}^*$, the absorption intensity of $C_{60}^{\bullet-}$ at 1080 nm increased, reaching a maximum at about 15 μs. The decay of $^3C_{60}^*$ and the appearance of $C_{60}^{\bullet-}$ are proof of the electron-transfer process in which $C_{60}^{\bullet-}$ is produced via $^3C_{60}^*$ by accepting an electron from 1,8-DMN (Eq. (1)). Similar behavior was observed in the case of 1,4-DMN. By using of the molar absorption coefficient (ε_T) of $^3C_{60}^*$ at 740 nm (16000 M^{-1} cm^{-1}) [20], the initial maximum concentration of $^3C_{60}^*$ ($[^3C_{60}^*]_{max}$) produced by a laser pulse is calculated. The maximum concentration of $C_{60}^{\bullet-}$ ($[C_{60}^{\bullet-}]_{max}$) at ca. 10 μs was also determined using the reported molar extinction coefficients (ε_A) of $C_{60}^{\bullet-}$ (12,000 M^{-1} cm^{-1} [19] −18,300 M^{-1} cm^{-1} [21] at 1080 nm in benzonitrile).

For C_{70} in benzonitrile, a similar electron-transfer process was confirmed from 1,8-DMN to $^3C_{70}^*$ (980 nm) [22,23] yielding $C_{70}^{\bullet-}$ (1380 nm) [24–26] as shown in Fig. 3. The transient absorption spectra for C_{60}/1,4-DMN or C_{70}/1,4-DMN are similar to those for 1,8-DMN. $[^3C_{70}^*]_{max}$ and $[C_{70}^{\bullet-}]_{max}$ were calculated using the reported ε_A value (6500 M^{-1} cm^{-1} at 980 nm) [19] and ε_A value (400 M^{-1} cm^{-1} at 1380 nm) [24], respectively.

$$^3C_{60}^*/^3C_{70}^* + \mathrm{DMN} \underset{\Phi_{et}^T}{\overset{k_{et}}{\rightarrow}} C_{60}^{\bullet-}/C_{70}^{\bullet-} + \mathrm{DMN}^{\bullet+} \quad (1)$$

It is worth mention that the decay of $^3C_{60}^*$ and rise of $C_{60}^{\bullet-}$ occur within 15 μs (inset of Fig. 2), which provides unambiguous evidence for electron transfer event via $^3C_{60}^*$. This is supported by admitting the oxygen into underlying the solutions where an intermolecular energy-transfer from $^3C_{60}^*$ to oxygen emerges, suppressing the electron transfer event.

Contrary to 1,4-DMN and 1,8-DMN, 2,7-DMN shows less effective electron transfer process to C_{60} and C_{70}. The

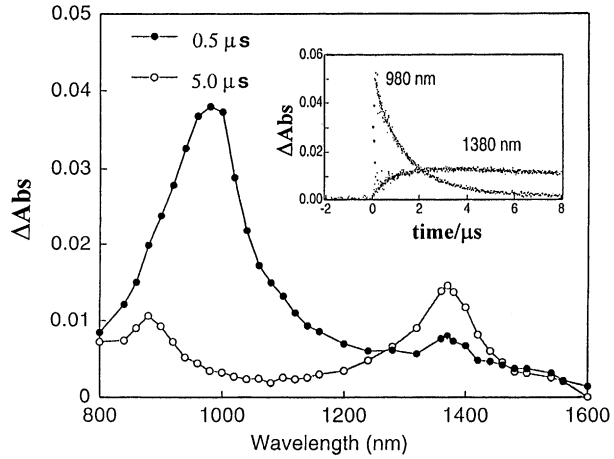

Fig. 3. Transient absorption spectra obtained by 532 nm laser photolysis of C_{70} (0.1 mM) in the presence of 1,8-DMN (20 mM) in Ar-saturated benzonitrile. Inset shows time profiles.

decay of $^3C^*_{60}$ and $^3C^*_{70}$ occurs as slow as about 80 μs and the absorption intensity of the radical anion was low as shown in Fig. 4. Fig. 4A displays the transient absorption spectra of C_{60} (0.1 mM) in the presence of 2,7-DMN (20 mM) in deaerated benzonitrile. Fig. 4B reveals that the decay of $^3C^*_{60}$ and the rise of $C_{60}^{\bullet-}$ were slightly enhanced by addition of Py. In the case of 2,3-DMN neither the rise of $C_{60}^{\bullet-}/C_{70}^{\bullet-}$ nor the decay of $^3C^*_{60}/^3C^*_{70}$ was observed even in the presence of Py, indicating that electron transfer via $^3C^*_{60}/^3C^*_{70}$ does not occur.

The effects of the concentration of DMN ([DMN]) on the kinetic behavior of transient species are studied (see Fig. 5). It is evident that the rates of decay of $^3C^*_{60}$-absorption and the subsequent rise rates of $C_{60}^{\bullet-}$ are significantly increased with increasing [DMN]. The analysis of the data in terms of the single exponential decay and single exponential rise yields the first-order rates of decay and rise (k_{1st}). The second-order rate constant k_q was obtained by plotting k_{1st} (for decay) versus [DMN]. Also, the second-order rate constant k_A (where subscript A represents $C_{60}^{\bullet-}$) was obtained by plotting k_{1st} for rise versus [DMN]. The obtained k_A values are in a good agreement with the corresponding k_q values within the experimental errors.

The efficiency of electron transfer via $^3C^*_{60}$ or $^3C^*_{70}$ can be estimated by the quantity $[C_{60}^{\bullet-}]/[^3C^*_{60}]$ (or $[C_{70}^{\bullet-}]/[^3C^*_{70}]$) as evaluated by the maximal and initial absorbance and reported ε_A and ε_T. The dependence of $[C_{60}^{\bullet-}]/[^3C^*_{60}]$ on [DMN] in benzonitrile is demonstrated in Fig. 6. It is evident that the efficiencies increase with [DMN] reaching a plateau, from which the quantum yield (Φ_{et}^T) for electron transfer via $^3C^*_{60}$ was estimated (Table 1). The Φ_{et}^T values for C_{70} were obtained similarly.

The rate constant for electron transfer (k_{et}) can be evaluated from the relation $k_{et} = \Phi_{et}^T \times k_q$ [5,26]. It should be noted that for 2,3-DHN (in the presence of Py), 1,8-DAN and 2,3-DAN, the k_{et} values (Table 1) are near the diffusion

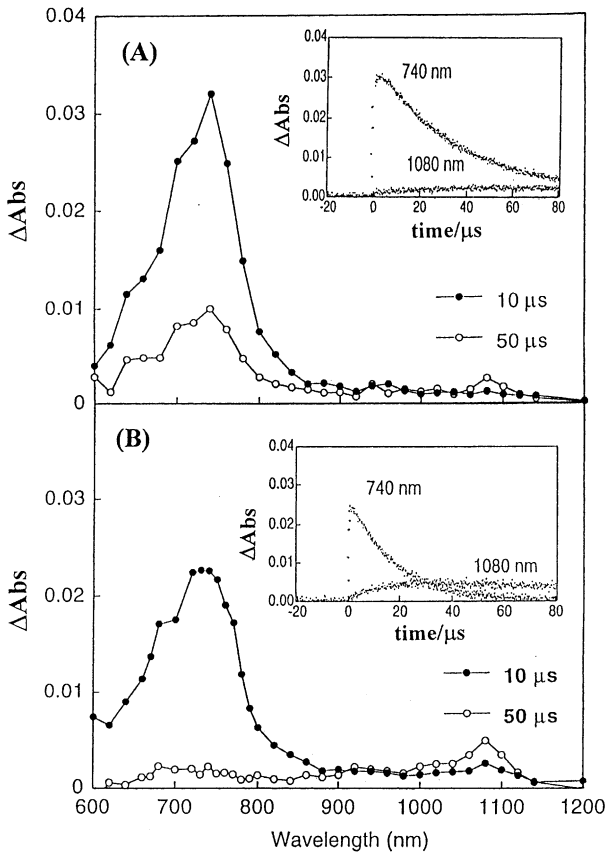

Fig. 4. Transient absorption spectra obtained by 532 nm laser photolysis of C_{60} (0.1 mM) in the presence of 2,7-DMN (20 mM) in Ar-saturated benzonitrile: (A) in the absence of Py and (B) in the presence of Py (0.5 M). Inset shows time profiles.

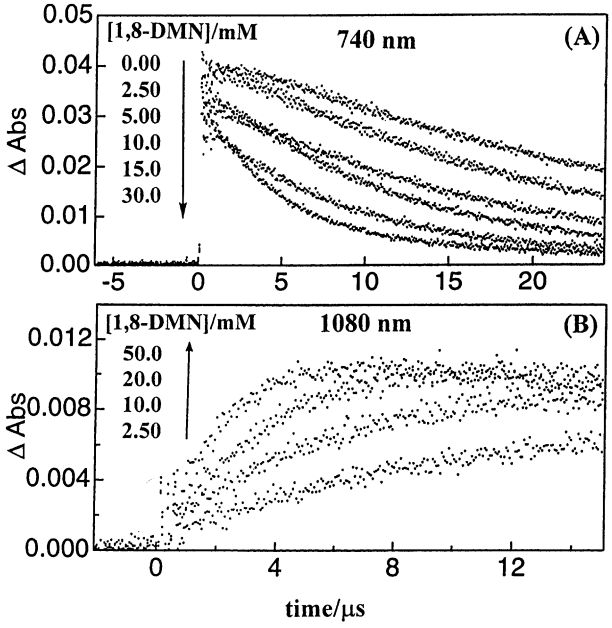

Fig. 5. (A) Decay profiles of $^3C^*_{60}$ at 740 nm with changing [1,8-DMN]. (B) Rise porofiles of $C_{60}^{\bullet-}$ at 1080 nm with changing [1,8-DMN].

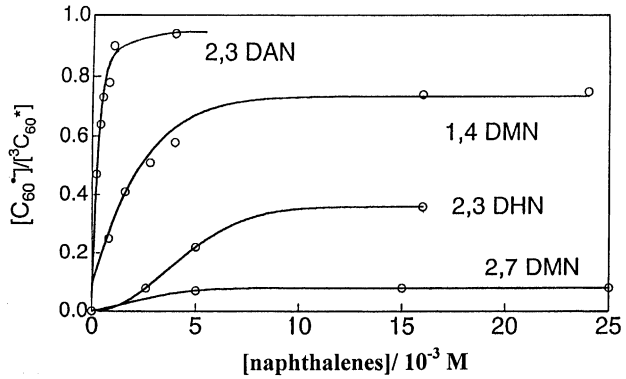

Fig. 6. Dependence of $[C_{60}^{\bullet -}]/[^3C_{60}^*]$ on [naphthalenes] in benzonitrile.

controlled limit ($k_{diff} = 5.6 \times 10^9\ M^{-1}\ s^{-1}$ in benzonitrile) [27].

The difference in the k_{et} values for dihydroxy-naphthalene in the absence and presence of Py can be explained as due to the interaction between $^3C_{60}^*/^3C_{70}^*$ and the hydrogen bonded DHN–Py complex, in which electron transfer from the DHN to $^3C_{60}^*/^3C_{70}^*$ is concerted with proton transfer from DHN to hydrogen bonded pyridine [5,8].

As can be seen from Table 1, effect of Py in the DMN is far less than that of DHN. The k_{et} values for 2,3-DHN are about three order of magnitudes larger than those observed for 2,7-DMN with C_{60}/C_{70}. The slight acceleration effect is attributed to the interaction of oxygen of the methoxy group with Py, which enhances the electron-donor ability of DMN.

As a matter of fact, we desire to find a significant pattern of electron transfer reactivity of α-substituted and β-substituted dimethoxy-naphthalenes towards $^3C_{60}^*/^3C_{70}^*$. In the latter case, slower reaction rates are obtained.

An explanation for the observed large k_{et} for 1,4-DMN and 1,8-DMN, in contrast to the much smaller value for 2,7-DMN, is to consider the oxidation potential values [28]. Because of their lower oxidation potentials 1,4-DMN (1.10 eV) and 1,8-DMN (1.17 eV) were expected to be better electron donors, where as 2,7-DMN (1.47 eV) was less efficient electron donor.

The free-energy change (ΔG_{et}) of the electron-transfer process from disubstitued-naphthalenes to $^3C_{60}^*/^3C_{70}^*$ can be calculated from the redox potentials of the donors $E_{1/2(oxid)}$ and the acceptor $E_{1/2(red)}$ and the lowest energy (E_{0-0}^*) of the triplet state of the acceptor according to Rehm–Weller relation [29]

$$\Delta G_{et} = E_{1/2(oxid)} - E_{1/2(red)} - E_{0-0}^* - C \quad (2)$$

ΔG_{et} was determined employing the lowest triplet energy of $^3C_{60}^*/^3C_{70}^*$ ($E_{0-0}^* = 1.45$–1.59 eV [30]), reduction potentials of C_{60}/C_{70} ($E_{1/2(red)} = -0.50$ V versus SCE [31]) and coulomb energy ($C = 0.06$ eV) in benzonitrile [12]. The resulting values of ΔG_{et} for mono- and disubstituted-naphthalene/fullerene systems are listed in

Table 1
Rate constants (k_q) for quenching of $^3C_{60}^*$ and $^3C_{70}^*$, quantum yields (Φ_{et}^T), electron transfer rate constants (k_{et}) and second-order back electron-transfer rate constant (k_{bet}^{2nd}) in benzonitrile

System	k_q ($M^{-1}\ s^{-1}$)[a]	Φ_{et}^T	k_{et} ($M^{-1}\ s^{-1}$)[b]	k_{bet}^{2nd} ($M^{-1}\ s^{-1}$)[c]
C_{60}/1-MN	2.72×10^5	0.17	4.6×10^4	6.50×10^9
C_{60}/2-MN	4.40×10^5	0.07	3.0×10^3	1.20×10^{10}
C_{60}/2,7-DMN/BN	1.17×10^5	0.08	8.8×10^3	1.02×10^{10}
C_{60}/2,7-DMN/Py/BN	6.60×10^5	0.10	6.6×10^4	1.30×10^{10}
C_{70}/2,7-DMN/BN	5.90×10^5	0.14	8.3×10^3	9.30×10^9
C_{70}/2,7-DMN/Py/BN	3.12×10^5	0.18	5.6×10^4	1.32×10^{10}
C_{60}/2,3-DMN/BN	_[d]	_[d]		_[d]
C_{60}/1,8-DMN/BN	4.4×10^6	0.49	2.2×10^6	2.30×10^{10}
C_{70}/1,8-DMN/BN	2.8×10^7	0.57	1.6×10^7	1.24×10^{10}
C_{60}/1,4-DMN/BN	2.6×10^8	0.76	2.0×10^8	3.00×10^{10}
C_{70}/1,4-DMN/BN	7.8×10^8	0.86	6.7×10^8	2.00×10^{10}
C_{60}/2,3-DHN/BN	1.5×10^6	0.23	3.5×10^5	1.30×10^{10}
C_{60}/2,3-DHN/Py/BN	1.6×10^9	1.00	1.5×10^9	1.80×10^{10}
C_{70}/2,3-DHN/BN	2.9×10^6	0.49	1.4×10^5	1.60×10^{10}
C_{70}/2,3-DHN/Py/BN	1.2×10^9	1.00	1.2×10^9	5.20×10^{10}
C_{60}/2,3-DAN/BN	3.5×10^9	0.94	3.3×10^9	1.26×10^{11}
C_{70}/2,3-DAN/BN	3.2×10^9	0.95	3.0×10^9	7.60×10^{10}
C_{70}/2,3-DAN/BN:BZ (1:1)	4.0×10^9	0.50	2.0×10^9	1.26×10^{11}
C_{60}/1,8-DAN/BN	3.8×10^9	1.00	3.8×10^9	1.03×10^{10}
C_{60}/1,8-DAN/BN:BZ (1:1)	6.6×10^9	0.77	5.1×10^9	3.38×10^{10}
C_{70}/1,8-DAN/BN	2.5×10^9	0.94	2.4×10^9	

[a] Each value contains estimation error of ±5%.
[b] $k_{et} = k_q \times \Phi_{et}^T$.
[c] $\varepsilon_A = 12000\ M^{-1}\ cm^{-1}$ at 1080 nm for $C_{60}^{\bullet -}$ [19] and $\varepsilon_A = 4000\ M^{-1}\ cm^{-1}$ at 1380 nm for $C_{70}^{\bullet -}$ [24].
[d] Too small to observe;
Φ_{et}^T becomes small by a factor of 0.66 when ε_A value for $C_{60}^{\bullet -}$ of $18{,}300\ M^{-1}\ cm^{-1}$ [21] was employed and k_{bet}^{2nd} becomes larger by a factor of 1.5 when ε_A value for $C_{60}^{\bullet -}$ of $18{,}300\ M^{-1}\ cm^{-1}$ [21] was employed.

Table 2
Oxidation potentials $E_{1/2(oxid)}$ vs. SCE, energy of HOMO of the donors employed and free energy changes (ΔG_{et}) of the photoinduced electron transfer in benzonitrile

System	$E_{1/2(oxid)}$ vs. SCE (eV)[a]	ΔG_{et} (kJ mol^{-1})	Energy of HOMO[b]
C_{60}/1-MN	1.38	30.88	0.538
C_{60}/2-MN	1.52	44.38	0.581
C_{60}/2,7-DMN	1.47	39.56	0.555
C_{70}/2,7-DMN	1.47	44.38	0.555
C_{60}/1,8-DMN	1.17	6.64	0.445
C_{70}/1,8-DMN	1.17	10.61	0.445
C_{60}/1,4-DMN	1.10	3.86	0.452
C_{70}/1,4-DMN	1.10	8.68	0.452
C_{60}/2,3-DHN	1.26[c]	19.30	0.486
C_{70}/2,3-DHN	1.26[c]	24.12	0.486
C_{60}/2,3-DAN	0.96[c]	−9.65	0.362
C_{70}/2,3-DAN	0.96[c]	−4.82	0.362
C_{60}/1,8-DAN	0.90[c]	−15.44	0.359
C_{70}/1,8-DAN	0.90[c]	−10.61	0.359

[a] From [26].
[b] Estimated from $E_{1/2(oxid)} = Ip - 6.7 \pm 0.1$ V (Ip is ionization potential) [33].
[c] For the details of the calculation, see [35].

Table 2. The positive values of ΔG_{et} indicate that probability of occurrence of electron transfer from dimethoxy- and dihydroxy-naphthalenes (in absence of Py) to $^3C^*_{60}/^3C^*_{70}$ is small. The ΔG_{et} (via $^3C^*_{60}/^3C^*_{70}$) for 1,8-DAN and 2,3-DAN is far negative, suggesting that k_{et} via $^3C^*_{60}/^3C^*_{70}$ should be close to the diffusion-controlled limit (k_{diff}). Fig. 7 presents a plot of $\log k_q$ in benzonitrile as a function of ΔG_{et}. The solid line was calculated using the usual kinetic scheme for electron transfer quenching processes in solution and the parameters reported by Rehm and Weller for the quenching of several aromatic molecules by electron donors [32]. Dimethoxy- and dihydroxy-naphthalenes (in absence of Py) show deviation from the plot.

Among the factors which may be responsible for the high electron transfer efficiency observed for α-substituted-naphthalenes compared with β-substituted naphthalenes, the fact that the intramolecular charge (electron) transfer character from α-position to the naphthalene ring is larger than that from β-position may be important [34], which is probably because of higher electron density of highest occupied molecular orbital (HOMO) at α-position than β-position. When the degree of the charge transfer is increased, the basicity of the aromatic nucleus is increased and the oxidation potential is decreased and hence the efficiency of electron transfer to $^3C^*_{60}/^3C^*_{70}$ should increase. Therefore, the values of k_{et} for 1,4-DMN and 1,8-DMN become greater than that for 2,7-DMN as shown in Table 1.

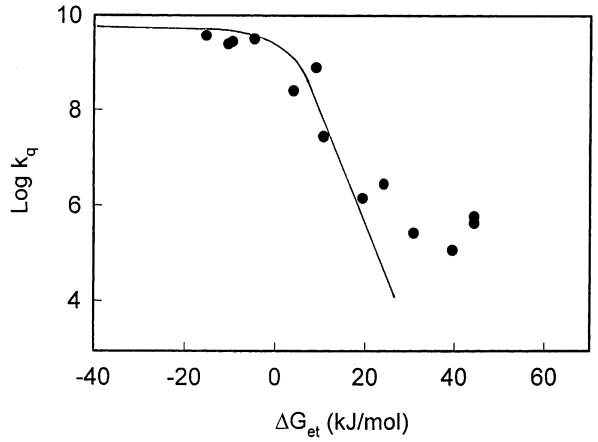

Fig. 7. Plot of $\ln k_q$ vs. ΔG_{et} for mono- and disubstituted-naphthalene/fullerene systems.

The behavior of the orbital energies in the α- and β-positions of the naphthalene may be understood in terms of the coefficients of atomic orbitals in the molecular orbitals of the parent naphthalene. The HOMO coefficients calculated by the HMO method [35] in the α-position of naphthalene exhibit a relatively high value (0.425) compared with the corresponding β-position (0.263). As a result, substitution at α-position of naphthalene should decrease the oxidation potentials as shown in Table 2. Therefore, the electron-donating properties of the substituents to naphthalene should penetrate through the carbon at α-position of naphthalene more than that through the β-position, increasing the donor ability of the naphthalene π-systems.

In the case of C_{60}/C_{70}-1,8-DAN/2,3-DAN systems a similar photoinduced electron transfer is observed. A significant high Φ^T_{et} values were observed compared with analogues dimethoxy-naphthalenes. As can also be seen from Table 1, the observed Φ^T_{et} values in bezonitrile are 0.94–1.0 for C_{60}/C_{70}-1,8-DAN/2,3-DAN systems, indicating high electron donor ability for 1,8-DAN and 2,3-DAN. We believe that the amino substituents may destabilize very much the HOMO energy and this is reflected in their low oxidation potential values as shown in Table 2. The HOMO energies for the mono and disubstituted-naphthalene (Table 2) are calculated by HMO method using Streitwieser's table values [35].

In a less polar solvent (1:1 mixture of benzonitrile to benzene, BN/BZ (1:1)), the transient absorption spectra for C_{60}/C_{70}-1,8-DAN/2,3-DAN displayed much the same features as in benzonitrile. The main difference includes the low intensity of $C_{60}^{\bullet-}/C_{70}^{\bullet-}$ relative to that of $^3C^*_{60}/^3C^*_{70}$, indicating slightly lower Φ^T_{et} than those in benzonitrile (Table 1). On the other hand, a faster decay rate of $^3C^*_{60}/^3C^*_{70}$ and the faster rise of $C_{60}^{\bullet-}/C_{70}^{\bullet-}$ in less polar solvent yielded larger k_q and k_A values; the k_{et} values obtained by multiplying Φ^T_{et} are listed in Table 1. A similar behavior was also observed in our previous paper [8].

3.3. Back electron transfer

Fig. 8 displays the time profile of $C_{60}^{\bullet-}$ on the long time-scale. It should be noted that the anion radicals begin to decay slowly after reaching each maximum. This can be attributed mainly to the back electron transfer from $C_{60}^{\bullet-}/C_{70}^{\bullet-}$ to $DMN^{\bullet+}/DHN^{\bullet+}$.

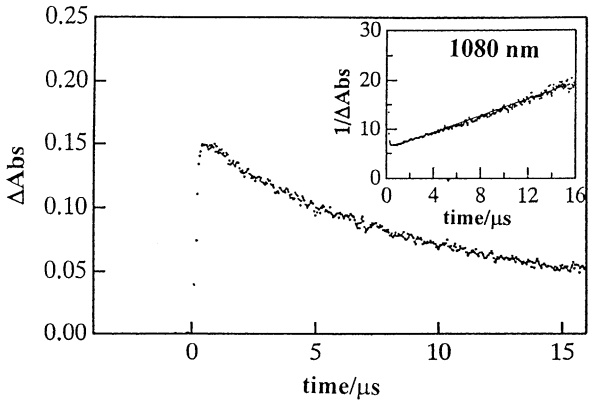

Fig. 8. Decay profile over long time scale of $C_{60}^{\bullet -}$ in the presence of 1,8-$DAN^{\bullet +}$ in benzonitrile. Inset shows second-order plot.

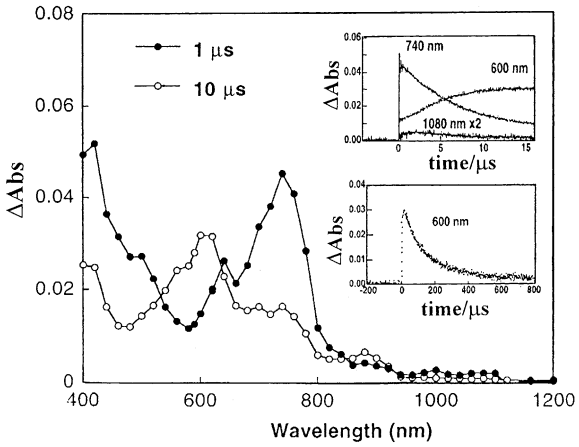

Fig. 9. Transient absorption spectra obtained by 532 nm laser photolysis of C_{60} (0.1 mM) in the presence of 1,8-DMN (20 mM) and OV^{+2} (0.4 mM) in Ar-saturated benzonitrile. Inset shows time profiles.

The decay time profiles obey second-order kinetics suggesting that the back electron transfer takes place between the free ion radicals [36]. From the slope of the second-order plot in the inset of Fig. 8, k_{bet}/ε_A was evaluated. The back electron-transfer rate constants (k_{bet}) were evaluated by substituting the reported ε_A values as listed in Table 1. It should be noted that the k_{bet} values generally decrease with increasing solvent polarity, owing to the strong solvation of the ion radicals in more polar solvents. In benzonitrile, the values of k_{bet} are close to the diffusion-controlled limit. The back-electron transfer may occur within a solvent-separated ion pair in BN/BZ (1:1), thus the k_{bet} values are larger than the k_{diff} values.

For 2,3-DHN in the presence of Py, on the other hand, the initial decays of $C_{60}^{\bullet -}/C_{70}^{\bullet -}$ obey first-order kinetics, suggesting that the back electron transfer takes place within the ion radical bridged via Py [9]. In the latter stage, this type of complex may dissociate in to the free radicals; thus, the later part of the decay is consistent with the second-order back electron transfer in the absence of Py. However, such a two-step-decay of $C_{60}^{\bullet -}/C_{70}^{\bullet -}$ was not observed for DMN's.

3.4. Electron-mediation process from $C_{60}^{\bullet -}/C_{70}^{\bullet -}$ to OV^{2+}

To investigate the electron mediation process after the photoinduced electron-transfer process, we measured the transient absorption spectra of C_{60} excited at 532 nm in the presence of both 1,8-DMN and OV^{2+} (0.4 mM) in deaerated benzonitrile solution (Fig. 9). The observed transient absorption bands at 740 and 1080 nm were attributed to $C_{60}^{\bullet -}$ and $^3C_{60}^*$, respectively, and the new band appeared at 600 nm may be attributed to $OV^{\bullet +}$, while the absorption band appeared at 420 nm can be assigned to the 1,8-$DMN^{\bullet +}$ [37].

The observed time profiles of the absorption bands are shown in the inset of Fig. 9. It is evident that the decay curve at 740 nm is accompanied with a concomitant rise of 1080 nm, which decays slowly with the rise of 600 nm

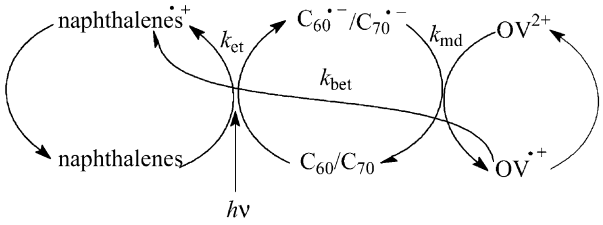

Scheme 1.

band. This implies that electron-mediaton (k_{md}) occurs from $C_{60}^{\bullet -}$ to OV^{2+} to regenerate C_{60} and $OV^{\bullet +}$. As can also be seen from the inset of Fig. 9, $OV^{\bullet +}$ at 600 nm begins to decay after reaching a maxima. The decay time profile obeys second-order kinetics, which implies that back electron transfer (k_{bet}) takes place from $OV^{\bullet +}$ to 1,8-$DMN^{\bullet +}$ to regenerate 1,8-DMN and OV^{2+}. From the slope of the second-order plot, k_{bet}/ε can be obtained. Upon substituting ε value of $OV^{\bullet +}$ (17,200 $M^{-1}\,cm^{-1}$ at 600 nm in benzonitrile) [38] the k_{bet} value was evaluated to be $5.9 \times 10^9\,M^{-1}\,s^{-1}$. The electron-mediation cycle is illustrated in Scheme 1.

4. Summary

The nature and position of substituents play a significant role on the quantum yields (Φ_{et}^T) and rate constants (k_{et}) of photoinduced electron transfer from $^3C_{60}^*/^3C_{70}^*$ to disubstituted-naphthalenes. There is a noticeable difference in the Φ_{et}^T and k_{et}, caused by substitutions at α- and β-positions, because the α-position of naphthalene exhibits relatively high electron density compared with the corresponding β-position. Therefore, substitution at α-position of naphthalene should decrease the oxidation potentials. Rehm–Weller behavior is observed in the plot of $\log k_q$

versus ΔG_{et}. In the presence of pyridine, the electron transfer efficiency for dihydroxy-naphthalene increased effectively but slightly for dimethoxy-naphthalenes. However, the transient absorption spectra of C_{60} in the presence of octylviologen and 1,8-DMN show that electron-mediaton occurs from $C_{60}^{\bullet -}$ to OV^{2+} to generate $OV^{\bullet +}$.

References

[1] R.J. Sension, A.Z. Szarka, G.R. Smith, R.M. Hochstrasser, Chem. Phys. Lett. 185 (1991) 179.
[2] J.W. Arbogast, C.S. Foote, J. Am. Chem. Soc. 113 (1991) 8886.
[3] L. Biczók, H. Linschitz, Chem. Phys. Lett. 195 (1992) 339.
[4] D.M. Guldi, H. Hungerbuhler, E. Janata, K.-D. Asmus, J. Chem. Soc. Chem. Commun. (1993) 84.
[5] L. Biczók, N. Gupta, H. Linschitz, J. Am. Chem. Soc. 119 (1997) 12601.
[6] L. Biczók, H. Linschitz, J. Phys. Chem. 99 (1995) 1843.
[7] N. Gupta, H. Linschitz, L. Biczók, Fullerene Sci. Technol. 5 (1997) 343.
[8] M. El-Kemary, M. Fujitsuka, O. Ito, J. Phys. Chem. A 103 (1999) 1329.
[9] M. El-Kemary, M. El-Khouly, M. Fujitsuka, O. Ito, J. Phys. Chem. A 104 (2000) 1196.
[10] M. El-Kemary, Can. J. Appl. Spectrosc. 41 (1996) 81.
[11] T. Konishi, Y. Sasaki, M. Fujitsuka, Y. Toba, H. Moriyama, O. Ito, J. Chem. Soc., Perkin Trans. 2 (1999) 551.
[12] J.W. Arbogast, C.S. Foote, C.S. Kao, J. Am. Chem. Soc. 114 (1992) 2277.
[13] S. Nonell, J. Arbogast, C.S. Foote, J. Phys. Chem. 96 (1992) 4169.
[14] Y. Sasaki, M. Fujitsuka, A. Watanabe, O. Ito, J. Chem. Soc., Faraday Trans. 93 (1997) 4275.
[15] T. Nojiri, M.M. Alam, H. Konami, A. Watanabe, O. Ito, J. Phys. Chem. A 101 (1997) 7943.
[16] T. Kato, T. Kodama, T. Shida, T. Nakagawa, Y. Matsui, S. Suzuki, H. Shiromaru, K. Yamauchi, Y. Aciba, Chem. Phys. Lett. 180 (1991) 446.
[17] M.A. Greaney, S.M. Gorun, J. Phys. Chem. 96 (1991) 7142.
[18] Z. Gasyna, L. Andrews, P.N. Schtz, J. Phys. Chem. 96 (1992) 1525.
[19] D.M. Guldi, H. Hungerbuhler, E. Janata, K.-D. Asmus, J. Phys. Chem. 97 (1993) 11258
[20] J.W. Arbogast, F.N. Diederich, M.M. Alvarez, S.J. Anz, R.L. Whetten, J. Phys. Chem. 95 (1991) 11.
[21] C.A. Steren, H. van Willigen, L. Biczók, N. Gupta, H. Linschitz, J. Phys. Chem. 100 (1996) 8920.
[22] R.M. Fraelich, R.B. Weisman, J. Phys. Chem. 97 (1993) 11145.
[23] H.T. Etheridge, R.B. Weisman, J. Phys. Chem. 99 (1995) 2782.
[24] D.R. Lawson, D.L. Feldheim, C.A. Foss, P.K. Dorhout, C.M. Elliott, C.R. Martin, B. Parkinson, J. Phys. Chem. 96 (1992) 7175.
[25] H. Hase, Y. Miyataka, Chem. Phys. Lett. 215 (1993) 141.
[26] M.M. Alam, A. Watanabe, O. Ito, J. Photochem. Photobiol. A: Chem. 104 (1997) 59.
[27] S.L. Murov, I. Carmichael, G.L. Hig, Handbook of Photochemistry, Marcel Dekker, New York, 1993.
[28] A. Zweig, A.H. Maurer, B.G. Roberts, J. Org. Chem. 32 (1967) 1322.
[29] D. Rehm, A. Weller, Isr. J. Chem. 8 (1970) 259.
[30] R.R. Hung, J.J. Grabowski, J. Phys. Chem. 95 (1991) 6073.
[31] P.M. Allemand, A. Koch, F. Wudl, Y. Rubin, F. Diederich, M.M. Alvarez, S.J. Anz, R.L. Whetten, J. Am. Chem. Soc. 113 (1991) 1050.
[32] D. Rehm, A. Weller, Ber. Bunsenges. Phys. Chem. 73 (1969) 834.
[33] R.E. Föll, H.E. Kramer, U.E. Steiner, J. Phys. Chem. 94 (1990) 276.
[34] H. Shizuka, S. Tobita, J. Am. Chem. Soc. 104 (1982) 6919.
[35] A. Streitwieser Jr., Molecular Orbital Theory For Organic Chemists, Wiley, New York, NY, 1961.
[36] O. Ito, Y. Sasaki, Y. Yoshikawa, A. Watanabe, J. Phys. Chem. 99 (1995) 9838.
[37] F. Quina, Z. Hamlet, F. Carroll, J. Am. Chem. Soc. 99 (1977) 2240.
[38] A. Harriman, A. Mills, J. Chem. Soc., Faraday Trans. 2 77 (1981) 2111.